# THE ISOFORMS OF RAT NATURAL KILLER CELL RECEPTOR NKR-P1 DISPLAY A DISTINCT BINDING OF COMPLEX SACCHARIDE LIGANDS

Ondřej PLÍHAL[a1,b], Pavla BYRTUSOVÁ[a2], Jiří PAVLÍČEK[a3], Ľuboslav MIHÓK[b1], Rüdiger ETTRICH[c], Petr MAN[a4,b], Petr POMPACH[a5,b], Vladimír HAVLÍČEK[b2], Lucie HUŠÁKOVÁ[b3] and Karel BEZOUŠKA[a6,b,*]

[a] *Department of Biochemistry, Faculty of Science, Charles University in Prague, Hlavova 8, 128 40 Prague 2, Czech Republic; e-mail: [1] plihal@biomed.cas.cz, [2] byrtusova @email.cz, [3] pavlicek @biomed.cas.cz, [4] pman@biomed.cas.cz, [5] pompach@biomed.cas.cz, [6] bezouska@biomed.cas.cz*

[b] *Institute of Microbiology, Academy of Sciences of the Czech Republic, Vídeňská 1083, 142 20 Prague 4, Czech Republic; e-mail: [1] luboslav.mihok@email.cz, [2] vlhavlic@biomed.cas.cz, [3] husakova@biomed. cas.cz*

[c] *Laboratory of High Performance Computing, Institute of Physical Biology, University of South Bohemia and Institute of Landscape Ecology, Academy of Sciences of the Czech Republic, Zámek 136, 373 33 Nové Hrady, Czech Republic; e-mail: ettrich@ greentech.cz*

Received June 27, 2003
Accepted September 27, 2003

*Dedicated to the 50th anniversary of the foundation of the Department of Biochemistry, the first biochemical department in Czechoslovakia.*

Lectin-like receptors of natural killer cells are critical for the regulation of their effector function. When these receptors are crosslinked with antibodies or multivalent ligands, they transmit either activating or inhibitory signals. Here we describe binding and inhibition experiments with recombinant extracellular ligand-binding domains of the rat NKR-P1A (activating) and NKR-P1B (inhibitory) receptors. We did not observe any difference in the binding of monosaccharide ligands by these receptors, but revealed dramatic differences in the binding of oligosaccharides and glycodendrimers. Our results explain the immunostimulatory effects of the glycodendrimers, which bind exclusively to the activating NKR-P1A isoform.

**Keywords**: Receptors; Carbohydrates; Oligosaccharides; Glycodendrimers; Ligands; Signaling; Lymphocyte; Lectins; NK cells.

Effector functions of natural killer lymphocytes, such as their ability to kill malignantly transformed, virally infected, or stressed cells, are regulated by activating or inhibitory signals, which are transmitted from receptors of ei-

ther immunoglobulin or lectins families[1,2]. Normal cells of the body are not killed by natural killer cells since they express high concentrations of MHC class I molecules[+] on their surface. These molecules are recognized by inhibitory receptors providing a dominant negative signal[3]. Activation receptors necessary to initiate the killing of malignant or other cells with low MHC class I expression have been much less studied. We investigated an activation receptor of rat natural killer cells, NKR-P1A, and showed its unique ability to activate the tumor cell lysis after crosslinking with antibodies, or specific carbohydrate ligands[4–6]. Recently, NKR-P1B receptor, which is evolutionarily closely related to NKR-P1A, has been shown to play an opposite role in both mouse and rat natural killer cells, where it transmits inhibitory signals[7–9]. Since we were not able to see any inhibitory effects of the carbohydrate ligands for NKR-P1A on natural killer cells or natural killing in the rat or mouse, we decided to express both isoforms from the rat and compare their carbohydrate binding properties.

## EXPERIMENTAL

### Chemicals

All carbohydrates were of D-configuration except for L-fucose. All monosaccharides, chitotetraose (G4), and $GlcNAc_{17}BSA$ were from Sigma. The preparation of chitotetraose was described previously[10]. The purity of all carbohydrates was checked by quantitative monosaccharide analysis as described by Dionex Corporation (Dionex Application Note 122). The preparation of glycodendrimers of poly(amidoamine) and polylysine type (see Scheme 1 for chemical structures of these compounds) was previously described[11,12]. The purity and integrity of these compounds was checked by quantitative carbohydrate analysis using colorimetric procedures, and MALDI mass spectrometry, respectively[13]. For inhibition tests, stock solutions in MilliQ water were prepared, checked by quantitative carbohydrate analyses, and adjusted to 2 mM concentrations. These stock solutions were stored in aliquots at –80 °C, and were stable for at least one year. All other chemicals were analytical grade reagents of the highest purity commercially available.

+ *Abbreviations used*: Bp, base pair; BSA, bovine serum albumin; MALDI, matrix-assisted laser desorption ionization; MHC, major histocompatibility complex; NK, natural killer; NKR-P1, natural killer receptor protein 1; PBS, phosphate buffered saline (10 mM sodium phosphate buffer (pH 7.4) with 150 mM NaCl); PCR, polymerase chain reaction; PVDF, poly(vinylidene difluoride); RT, reverse transcription. A single-letter code was used for the description of amino acids.

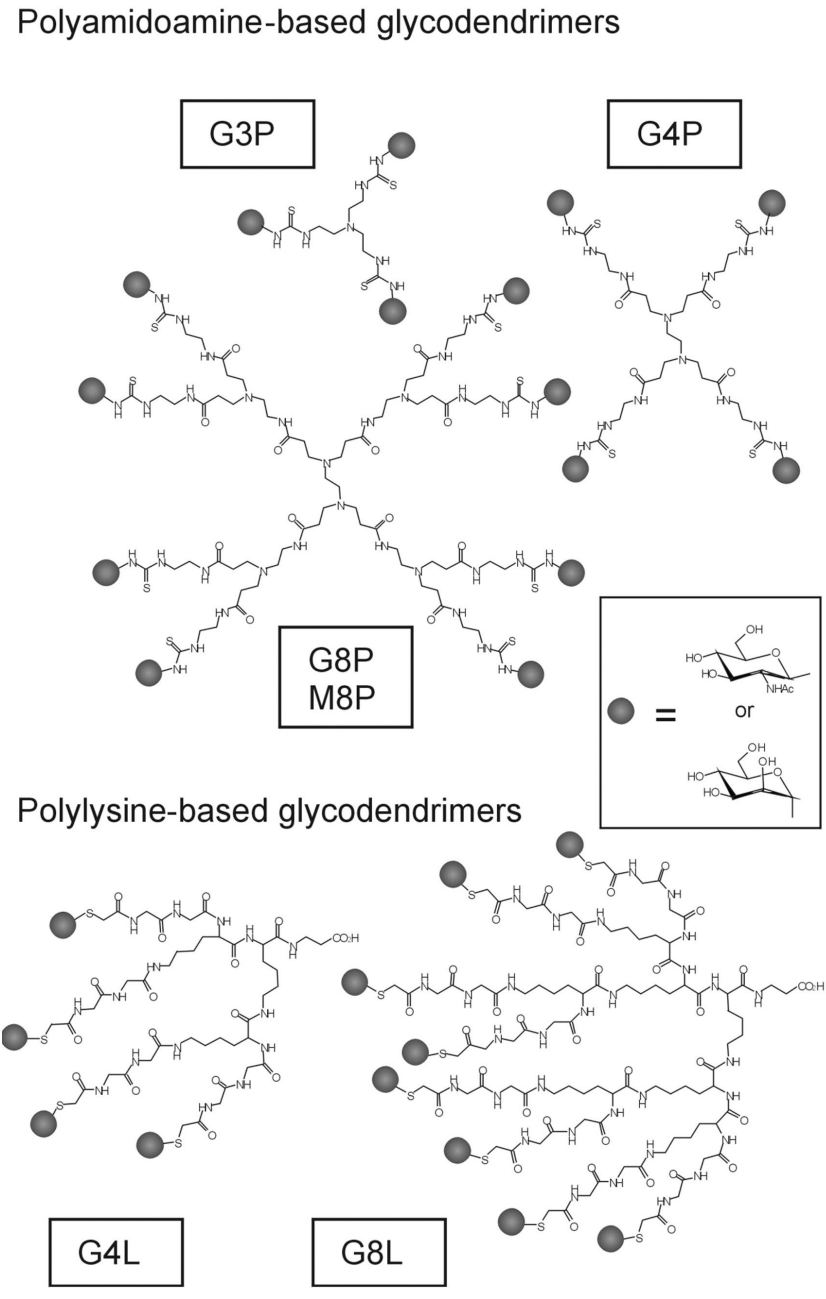
Polyamidoamine-based glycodendrimers
G3P
G4P
G8P
M8P
=
or
Polylysine-based glycodendrimers
G4L
G8L

SCHEME 1

Preparation of Recombinant NKR-P1A and NKR-P1B Proteins

Recombinant NKR-P1A protein was prepared as described previously using pET-30a bacterial expression vector[14a,14b]. In order to amplify the DNA fragment coding for the NKR-P1B isoform, RT-PCR was performed with 5 μg of total RNA isolated from the cell line RNK-16 [5], 5′-TGGCTTTCACACCGAGAT-3′ as forward primer and 5′-CACAAGCTTTCATTTTAGTTCCTT-TTGACAGACCCA-3′ as reverse primer using the DeepVent DNA polymerase protocol (NEB). The resulting blunt-ended DNA fragment was ligated into pBluescript SK+ vector (Stratagene), and used for the subsequent subcloning by another PCR amplification with a forward primer 5′-AAATATCATATGTGGAGGGAAGTCTAGCTGAC-3′ and the same reverse primer as above. The blunt-ended DNA fragment obtained by the latter amplification was cloned in the same vector as above. Finally, the *Nde*I–*Hind*III fragment was excised by the respective restriction endonucleases, and transferred to pET-30a and pRSETB expression vectors (from Novagen and Invitrogen, respectively), which had been cut by the same enzymes and treated with alkaline phosphatase[14b]. The expression vectors were sequenced on both strands using the corresponding dye primers and automated DNA sequencer (ABI Prism 3100). The protein was produced in *Escherichia coli* strain BL-21 RIL (Stratagene) in cultures grown in 2 l of LB medium supplemented with the suitable antibiotics (either ampicillin or kanamycin together with tetracycline and chloramphenicol). Cultures were induced with 0.4 mM isopropyl thio-β-D-galactopyranoside, and grown for additional 5 h. Bacteria were harvested and inclusion bodies were prepared[15]. They were dissolved in 10 ml of 6 M guanidium hydrochloride and 10 mM dithiothreitol. NKR-P1A was refolded as described previously[14a], NKR-P1B was refolded by dropwise addition of above solution of inclusion bodies into 1 l of refolding buffer consisting of 50 mM Tris-acetate (pH 7.5) with 1 M L-arginine, 10 mM $CaCl_2$, 1 mM $NaN_3$, 5 mM cysteamine and 5 mM cystamine. The protein solution was stirred at 4 °C overnight, and dialyzed against 10 l of 10 mM Tris-HCl (pH 8.5) with 0.5 M NaCl and 1 mM $NaN_3$ for 24 h followed by dialysis against 10 l of 10 mM Tris-HCl (pH 8.5) with 49 mM NaCl and 1 mM $NaN_3$. The refolded protein was captured by chromatography on Q-Sepharose FF column (Amersham, 1.6 × 20 cm) equilibrated in the latter buffer. Protein was eluted with a linear gradient of NaCl, from 49 mmol $l^{-1}$ to 1 mol $l^{-1}$, for 60 min, and concentrated using Centriprep 3 and Centricon 3 devices. Final separation was performed on Superdex 200 HR 10/30 column (Amersham) equilibrated in 10 mM Tris-HCl (pH 7.5) with 120 mM NaCl and 1 mM $NaN_3$. The monomeric NKR-P1B protein was stored in this buffer concentrated to 10 mg/ml.

Analysis and Labeling of Recombinant NKR-P1A and NKR-P1B Proteins

The purity and identity of NKR-P1 proteins was evaluated using several methods. SDS electrophoresis, under both reducing and nonreducing conditions, was performed in the buffer system of Laemmli[16]. The separated proteins were also blotted onto PVDF membrane (Immobilone P, Millipore) and 10 cycles of automated Edman degradations (Protein Sequencer LF3600D, Beckman) were performed to verify the N-terminal sequence. Native size and monomeric status of the proteins were evaluated using gel filtration on Superdex 200 HR as described above. The correct size of the proteins was evaluated by MALDI mass spectrometry[17]. The correct type of disulfide bonding was checked by measuring the size of peptide fragments obtained after overnight digestion with pepsin (substrate:enzyme ratio 100:1) in 2% acetic acid by the same technique. The digested fragments were separated by reversed phase chromatography on Vydac C-18 column equilibrated in 0.1% TFA in water.

Elution was done with the gradient of acetonitrile increasing its concentration by 1% per min. NKR-P1A and NKR-P1B proteins were labeled biosynthetically using [$^{35}$S]-methionine, or externally using carrier-free Na[$^{125}$I] (both from Amersham) and the Iodogen (Pierce) protocol.

### Binding and Inhibition Assays

Binding of the radiolabeled recombinant proteins to microplate wells (Immunol 4, Dynatech) coated with $GlcNAc_{17}BSA$ was performed as described previously[4]. Briefly, for binding experiments 96 well plates were coated at 4 °C overnight with 50 µl of $GlcNAc_{17}BSA$ (10 µg/ml, Sigma) in PBS, washed three times with PBS, and blocked with 200 µl of 2% BSA in PBS at 4 °C for 2 h. Wells were filled with 100 µl of PBS containing approximately $10^4$ Bq of the radioiodinated protein (specific activity $10^5$ Bq/µg protein) adjusted to the total amount tested with the addition of nonlabeled protein. Plates were incubated at 4 °C for 2 h, washed three times with cold (4 °C) PBS, and dried. An amount of 100 µl of scintillation liquid was added into each well, and the radioactivity was determined by liquid scintillation counting (Microbeta, Wallac). Control wells for background subtraction were coated with BSA instead of $GlcNAc_{17}BSA$. Plate inhibition assays were performed at 50% saturation of binding in triplicate experiments[4] in the presence of the indicated inhibitor concentrations. Inhibitory potency of each compound was expressed as the concentration providing 50% inhibition under these experimental conditions ($IC_{50}$).

### Molecular Modeling

The procedures used for molecular modeling were very similar to those described previously[14b]. Briefly, the structures 1QO3 and 1B6E were extracted from the Brookhaven Protein Data Bank (http://www.pdb.org) and loaded into SYBYL 6.6.2 (Tripos Associates), where we performed homology modeling against the NKR-P1A sequence. Hydrogens were added and a Conolly-type surface with the electrostatic potential based on Gasteiger–Hückel partial charge distribution was calculated. Energy minimization was followed by molecular dynamics simulation at 290 K with the NTV ensemble over 15 000 fs. The resulting structure was then minimized with the same parameters as above to the convergence of the energy gradient less than 0.01 kJ $mol^{-1}$ $nm^{-1}$. The interaction with chitotetraose was studied using the AutoDock 3.0.3 program. For the explicit model of hydrogen bonds it was necessary to add polar hydrogen and assign partial atom charges to the macromolecule. Lamarckian genetic algorithm was used for docking. The selected docking positions were subjected to 2000 steps of steepest descent minimization optimizing both internal and relative geometries of the substrate and the binding site residues.

## RESULTS

### *Cloning and Expression of NKR-P1B*

DNA coding for NKR-P1B was first amplified by RT-PCR as a larger fragment using primers that were designed to distinguish both isoforms in a sequence showing a maximal number of differences. From this larger DNA

fragment, a smaller fragment coding for the part of molecule corresponding exactly to the extracellular globular ligand-binding domain (Fig. 1a) was subcloned. This DNA fragment coding 101 amino acids ($W_{115}$–$K_{215}$, Fig. 1b) was inserted into pET-30a and pRSETB expression vectors just after the initiation methionine necessary for correct protein translation. Both expression plasmids were transformed into the production bacterial strains, and trial induction experiments were performed. Interestingly, only the DNA fragment inserted into the pRSETB expression vector led to the successful production of protein. The overproduced protein was shown to precipitate in the inclusion bodies. Therefore, repeated large scale bacterial cultures were produced, and inclusion bodies were isolated as a source of protein for the refolding experiments.

a

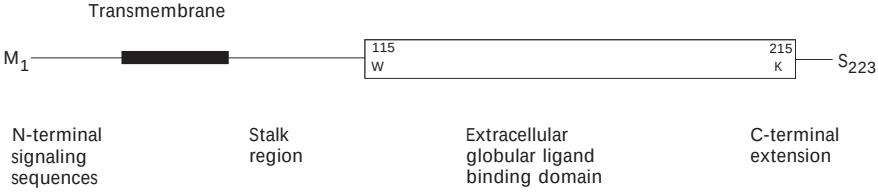


b

```
                                115                                                 164
NKR-P1B rat [gi27713280] WKGSLADCGGKGATLLLVQDQEELRFLRNLTKRISSSFWIGLSYTLSDEK
NKR-P1B rat [gi1354768]  WKGSLADCGGKGATLLLVQDQEELRFLRNLTKRISSFWIGLSYTLSDEK
NKR-P1A rat [gi128357]   WKESLADCGGKGATLLLVQDQEELRFLRNLTKRISSFWIGLSYTLSDEN
NKR-P1B mouse[gi13774945]WKECRIDCDKKGATLLLIQDQRRLRFLLDSIKEKYNSFWIGLSYTLTDMN

                    165                                                 215
NKR-P1B rat   WKWINGSTLNSDALNITGDTEKDSCASVSQDKVLSESCDSDNIWICQKELK
NKR-P1B rat   WKWINGSTLNSDALNITGDTEKDSCASVSQDKVLSESCDSDNIWICQKELK
NKR-P1A rat   WKWINGSTLNSDVLSITGDTEKDSCASVSQDKVLSESCDSDNIWVCQKELK
NKR-P1B mouse WKWINGTAFNSDVLKITGDTENGSCASISGDKVTSESCSTDNRWICQKELN
```

FIG.1

a Schematic representation of NKR-P1 receptor. This molecule is composed of the N-terminal intracellular signaling sequences, a transmembrane domain, a stalk region, the extracellular ligand-binding domain, and a short C-terminal extension. The proteins used here correspond to the ligand-binding part of the receptor, amino acids $W_{115}$ to $K_{215}$. b Multiple sequence alignments of the rat NKR-P1A receptor, two published sequences of the rat NKR-P1B receptors, and the mouse NKR-P1B. The GeneBank accession numbers of the respective clones are indicated in parentheses

*Refolding, Purification and Characterization of NKR-P1B*

Several protocols were tested for the optimal refolding of NKR-P1B, of which the procedure based on a rapid dilution provided the best yield of biologically active protein (data not shown). The correctly folded protein was recovered by anion exchange chromatography on Q-Sepharose. The protein after this procedure was mostly monomeric, and a small amount of aggregates and oligomers was removed by gel filtration. The recombinant NKR-P1B domain was stable for at least six months when stored as a concentrated solution at 4 °C. Lyophilization of the protein should be avoided since it resulted in precipitation of protein, and loss of its biological (carbohydrate binding) activity.

The final preparation of NKR-P1B was analyzed by several techniques. Denaturing electrophoresis in the presence of SDS provided an estimated molecular size of approximately 14 000 (Fig. 2a, lane 2), which was identical with that of NKR-P1A (Fig. 2a, lane 1). Under nonreducing conditions the mobility was somewhat slower, indicating the existence of different molecular species with the disulfide bridges (Fig. 2a, lane 3). Both NKR-P1A and NKR-P1B separated under reducing conditions were also blotted onto PVDF membrane, and the Coomassie Brilliant Blue R-250-stained blot was used for N-terminal sequencing. Ten cycles of automated Edman degradations provided sequences MWKESLADXG and MWKGSLADXG, respectively. This verified the identity of the proteins, and also indicated that processing of the N-terminus with the bacterial initiation methionine exopeptidase did not occur in either of the two proteins. The identity of the entire protein was further confirmed by peptide mass mapping after trypsin digestion, which provided sequence coverage of 57 and 75%, respectively. Finally, the entire mass of the refolded protein was checked by MALDI-MS, and the correct disulfide bonding within the molecule was verified by MALDI-MS analysis of the pepsin digests (an extensive data set for the latter analysis will be published elsewhere). Finally, the native size of the protein was determined by gel filtration, and found to be 12 600, confirming the monomeric status (Fig. 2b).

*Ligand-Binding and Ligand-Inhibiton Studies*

In order to establish the feasibility of the use of the previously employed plate binding and inhibition assays, we have performed saturation experiments using plastic microtiter plates coated with the high-affinity neoglycoprotein ligand, $GlcNAc_{17}BSA$. Moreover, in order to exclude any possi-

ble effects of the label attached to the protein on the binding, two protein radiolabeling protocols were employed: metabolic labeling using [$^{35}$S]-methionine, and external labeling by a standard protein iodination protocol with Na[$^{125}$I]. Both of these protocols resulted in efficient protein labeling to a specific activity of approximately $10^{11}$ Bq per mol of protein. Both labeling methods provided essentially identical binding results (shown in Fig. 3 for the radioiodinated protein). Moreover, binding of both NKR-P1A and NKR-P1B proteins to the ligand-coated wells followed very similar kinetics with saturation at approximately 2 μg of protein per well (Fig. 3).

These experiments were important for the design of subsequent inhibition studies. When monosaccharides were used as the inhibitors, both the

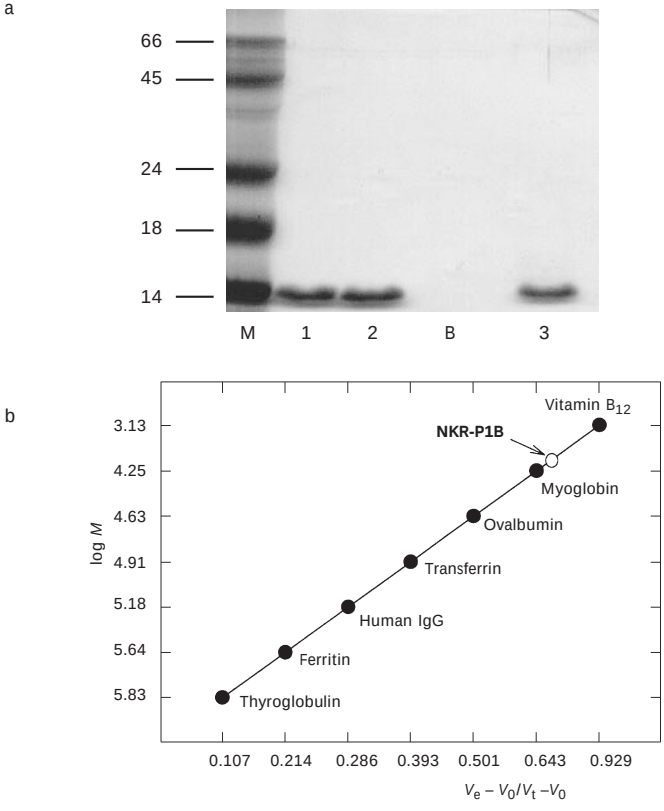


FIG. 2

Analysis of NKR-P1B protein by SDS electrophoresis (a) and gel filtration (b). Lanes in a were: M, protein molecular mass marker; 1, NKR-P1A, reducing conditions; 2, NKR-P1B, reducing conditions; 3, NKR-P1B, nonreducing conditions. Samples analyzed under reducing and nonreducing conditions are separated by a blank lane (B) containing the nonreducing buffer

hierarchy and values of $IC_{50}$ were indistinguishable between NKR-P1A and NKR-P1B for all the 6 sugars tested (Fig. 4a). The best monosaccharide ligand was in both cases ManNAc with $IC_{50}$ approximately $1 \times 10^{-8}$ mol $l^{-1}$. However, when we investigated the inhibitory potencies of various oligosacharides and clustered carbohydrates, we have found dramatic differences between their $IC_{50}$ values for NKR-P1A and NKR-P1B. These differences were the highest for the oligosaccharide ligand chitotetraose (Fig.4b, column G4). The affinities of NKR-P1B to the other investigated oligosaccharides and glycodendrimers were much lower than for NKR-P1A (Fig. 4b).

*Explanation of Binding Data Provided by Molecular Modeling*

The dramatic differences in binding of the complex oligosaccharide ligands by NKR-P1 isoforms were surprising in view of the closely related primary (and, possibly, three-dimensional) structure of both receptors. There are only 6 amino acid substitutions between the two proteins (shown in bold in Fig. 1b) which gives an amino acid identity of 93.1%. In order to provide a structural explanation for the binding data obtained here, we used molecular modeling to visualize the binding surface of NKR-P1A, and used this computed surface to dock the chitotetraose ligand. The results of these analyses (Fig. 5), and additional results not shown here[18], indicate clearly the existence of a ligand-binding groove for chitotetraose extending over the surface of the globular domain. This groove extends from the subsite

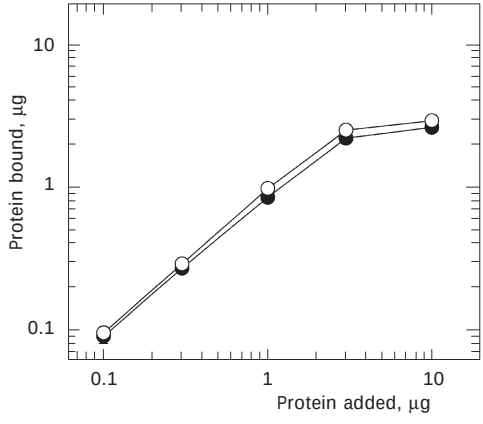


FIG. 3
Saturation curves for binding of NKR-P1A (●) and NKR-P1B (○) receptors to microtiter wells coated with the high-affinity ligand, $GlcNAc_{17}BSA$

for the nonreducing end of the chitotetraose in the membrane proximal region to the subsite for the reducing end in the membrane distal area. Our recent results indicate that the dominant subsite responsible for the binding of monosaccharides is in the position of nonreducing GlcNAc (literature[18], lower part of Fig. 5). Interestingly, this region of the receptor is essentially identical in both NKR-P1A and NKR-P1B. On the other hand, there are important amino acid substitutions starting from the region of the subterminal GlcNAc unit. Namely, $V_{177}$, which forms hydrophobic interactions with the *N*-acetyl in this particular carbohydrate, is replaced by $A_{177}$. Even

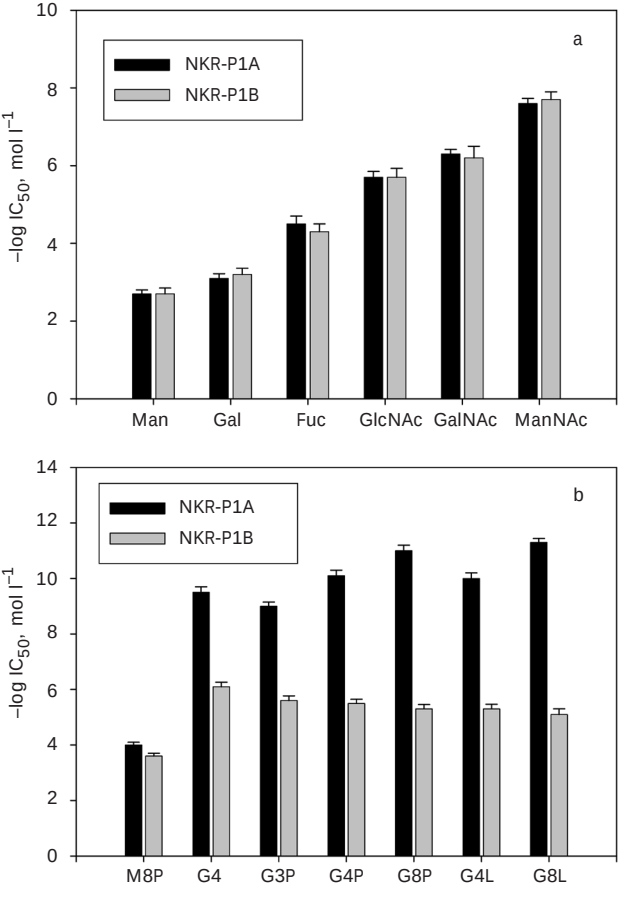


FIG. 4

Summary of the inhibition of binding of NKR-P1A and NKR-P1B receptors to $GlcNAc_{17}BSA$-coated wells by various monosaccharides (a) and complex carbohydrates (b). The values are represented as the mean ± S.D. calculated from three independent determinations

more importantly, $S_{179}$ in NKR-P1A is replaced by $N_{179}$ in NKR-P1B. This substitution is possibly responsible for the dramatic differences in the binding data. In the recombinant NKR-P1B protein, the much larger side-chain of $N_{179}$ when compared with the small OH group of $S_{179}$ probably causes a steric clash for the binding of complex oligosaccharides in this area. Interestingly, this effect would be even more dramatic in the native protein, because $N_{179}$ would be a part for the site of N-glycosylation. In this case the large oligosaccharide side-chain attached to the receptor in this position would essentially prevent the binding of the complex oligosaccharide ligands.

## DISCUSSION

The NK cell receptors NKR-P1 described here are type II membrane proteins expressed as homodimers at the cell surface. They expose their carbohydrate-binding domains into the extracellular environment while retaining their signal transducing sequences intracellularly. Since the binding of carbohydrates to these receptors would be much influenced by the oligomeric status of their carbohydrate-binding domains, we decided to use monomeric ligand-binding domains of both NKR-P1A and NKR-P1B. This selection was justified by unusually high affinity of NKR-P1A for carbohydrates[4,5], which allows to measure reliable binding data with this protein with no need to cluster its ligand-binding domain into higher-order dimers of oligomers[19].

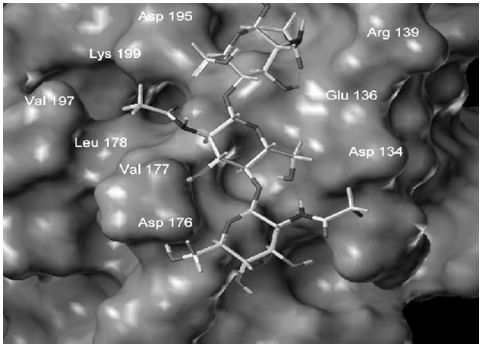


FIG. 5
Spatial view of the molecular model of the rat NKR-P1A with the chitotetraose docked into the oligosaccharide-binding groove. Important amino acids ligating the oligosaccharide are also indicated

NKR-P1B is a minor form among NKR-P1 receptors in the rat. It was first observed on Northern blots of mRNA extracted from the NK cell line RNK-16 and probed with the cDNA probe prepared from full-length rat NKR-P1A as a weaker, larger (1.7 kbp) band comprising about 5% of the total message for NKR-P1 family members[20]. Indeed, amplification of DNA fragment coding for this molecule proved difficult, especially since several initial attempts resulted in the amplification of the closely related NKR-P1A isoform that is prevalent in the starting material. We have eventually succeeded using a strategy in which somewhat larger DNA fragment coding for NKR-P1B was first amplified using primers against the region displaying the highest dissimilarity between NKR-P1A and NKR-P1B. Amplified DNA for NKR-P1B was checked by sequencing. Interestingly, while our sequence was essentially identical with a sequence deposited in the NCBI database and coming from the large-scale genome sequencing project (Fig. 1b, sequence[21] gi27713280), there was one amino acid difference when compared to the published sequence for rat NKR-P1B (Fig. 1b, sequence[22] gi1354768). Since this amino acid substitution ($S_{149} \rightarrow I_{149}$) is a result of difference in a single nucleotide (i.e. AGT → ATT), we believe that it may have been caused by a sequencing error.

Several refolding protocols were tried in order to find optimum conditions for the production of the native ligand-binding domain. Surprisingly, unlike in the case of NKR-P1A, rapid dilution of protein from denaturing solution provided the highest yield of the native protein. It was necessary to add 1 M L-arginine to prevent the precipitation of protein during the refolding. An optimal redox buffer, which consisted of 5 mM cysteamine and 5 mM cystamine was also required. Refolding proceeded for several hours in the cold (4 °C), and was followed by dialysis into a high salt (0.5 M NaCl) buffer. Such a step is important to lower the protein concentration, to facilitate the removal of the refolding reagents and simultaneously to stabilize the hydrophobic interactions within the small core of the protein domain in the high salt environment.

For the binding of oligosaccharides to NKR-P1A, the theory of the long "binding groove" into which the extended structure of the chitooligomers would accommodate became very useful[18]. This idea was supported by the fact of growing affinity to NKR-P1A in the series[23] GlcNAc → $(GlcNAc)_2$ → $(GlcNAc)_3$ → $(GlcNAc)_4$. In the case of NKR-P1B it seems that the architecture of the binding groove is disturbed in the way that sterically limits the interaction with the multivalent ligand. However, the basic arrangement of the unique binding sites for monosaccharides remains conserved (see Fig. 5). This interesting dichotomy of binding properties of both proteins

can be important for the understanding of the opposite functional roles of these proteins in the NK cell signaling. However, it should be emphasized that while the results reported here were obtained for the soluble monomeric ligand-binding domains, the native form of NKR-P1A and NKR-P1B receptors are dimeric. We have recently obtained soluble forms of the dimeric receptor proteins, and tested their binding activities for both monosaccharides and complex saccharides ligands. The conclusions of these studies (the results of which will be published elsewhere) seem to be in complete agreement with those obtained using the monomeric proteins. Thus, the numerous observations in our laboratory that the glycodendrimeric GlcNAc-bearing ligands have always activating effects on NK cells would be consistent with the the results reported here. These observations also allow to understand why NKR-P1A seems to be one of the most important receptors for the glycodendrimers in vitro, and in vivo[24,25].

## CONCLUSIONS

We have shown here that rat NKR-P1B, a new inhibitory receptor of NK cells, had the same affinity to a unique set of monosaccharide ligands as rat NKR-P1A, which is an activating receptor. The best monosaccharide ligand was ManNAc in both cases. However, the affinity of NKR-P1B to several oligosaccharides and glycodendrimers was much lower compared with that of NKR-P1A. We also provided a structural explanation for these observations based on molecular modeling. These results suggest a possible molecular mechanism for the opposite function of the two proteins on rat NK cells. Only the activating NKR-P1A receptor should be able to recognize its complex oligosaccharide ligands with sufficient affinity to result into immunologically important activation of NK cells and other subsets bearing this receptor. On the other hand, the ligand initiating the inhibition of natural killing through engagement of NKR-P1B remains to be identified.

*The financial support provided by the Grant Agency of the Czech Republic (grant No. 203/01/1018) is gratefully acknowledged.*

## REFERENCES

1. Yokoyama W. M.: *Curr. Biol.* **1995**, *5*, 982.
2. Weis W. I., Taylor M. E., Drickamer K.: *Immunol. Rev.* **1998**, *163*, 19.
3. Yokoyama W. M.: *Curr. Opin. Immunol.* **1995**, *7*, 110.
4. Bezouška K., Vlahas G., Horváth O., Jinochová G., Fišerová A., Giorda R., Chambers W. H., Feizi T., Pospíšil M.: *J. Biol. Chem.* **1994**, *296*, 16945.

5. Bezouška K., Yuen C.-T., O'Brien J., Childs R. A., Chai W., Lawson A. M., Drbal K., Fišerová A., Pospíšil M., Feizi T.: *Nature* **1994**, *372*, 150.
6. Pospíšil M., Vannucci L., Horváth O., Fišerová A., Krausová K., Bezouška K., Mosca F.: *Int. J. Oncol.* **2000**, *16*, 267.
7. Kung S. K. P., Su R. C., Shannon J., Miller R. G.: *J. Immunol.* **1999**, *162*, 5876.
8. Carlyle J. R., Martin A., Mehra A., Attisano L., Tsui F. W., Zuniga-Pflucker J. C.: *J. Immunol.* **1999**, *162*, 5917.
9. Li J., Rabinovich B. A., Hurren R., Shannon J., Miller R. G.: *Int. Immunol.* **2003**, *15*, 411.
10. Semeňuk T., Krist P., Pavlíček J., Bezouška K., Kuzma M., Novák P., Křen V.: *Glycoconjugate J.* **2001**, *18*, 817.
11. Lindhorst T. K., Kieburg C.: *Angew. Chem., Int. Ed. Engl.* **1996**, *35*, 1953.
12. Zanini D., Roy R.: *Bioconjugate Chem.* **1997**, *8*, 187.
13. Bezouška K., Křen V., Kieburg C., Lindhorst T. K.: *FEBS Lett.* **1998**, *426*, 243.
14. a) Pavlíček J., Bezouška K.: *Chem. Papers* **1998**, *52*, 327; b) Pavlíček J., Sopko B., Ettrich R., Kopecký V., Baumruk V., Man P., Havlíček V., Vrbacký M., Martínková L., Křen V., Pospíšil M., Bezouška K.: *Biochemistry* **2003**, *42*, 9295.
15. Valez-Gomez M., Reyburn H. T., Mandelboim M., Strominger J. L.: *Immunity* **1998**, *9*, 337.
16. Laemmli U. K.: *Nature* **1970**, *227*, 680.
17. Bezouška K., Sklenář J., Novák P., Halada P., Havlíček V., Kraus M., Tichá M., Jonáková V.: *Protein Sci.* **1999**, *8*, 1551.
18. Pavlíček J.: Unpublished results.
19. Bezouška K.: *J. Biotechnol.* **2002**, *90*, 269.
20. Ryan J. C., Niemi E. C., Nakamura M. C., Seaman W. E.: *J. Exp. Med.* **1995**, *181*, 1911.
21. Rat Genome Sequencing Consortium: http://hgsc.bcm.tmc.edu/projects/rat.
22. Dissen E., Ryan J. C., Seaman W. E., Fossum S.: *J. Exp. Med.* **1996**, *183*, 2197.
23. Bezouška K., Sklenář J., Dvořáková J., Havlíček V., Pospíšil M., Thiem J., Křen V.: *Biochem. Biophys. Res. Commun.* **1997**, *238*, 149.
24. Vannucci L., Fišerová A., Sadalapure K., Lindhorst T. K., Kuldová M., Rossman P., Horváth O., Křen V., Krist P., Bezouška K., Luptovcová M., Mosca F., Pospíšil M.: *Int. J. Oncol.* **2003**, *23*, 203.
25. Pospíšil M., Vannucci L., Fišerová A., Krausová K., Horváth O., Křen V., Mosca F., Lindhorst T. K., Sadalapure K., Bezouška K.: *Adv. Exp. Med. Biol.* **2001**, *495*, 343.